Astro2020 Science White Paper
proj Testing Gravity Using Type Ia Supernovae Discovered by Next-Generation Wide-Field Imaging Surveys

Thematic Areas: ☐ Planetary Systems   ☐ Star and Planet Formation
☐ Formation and Evolution of Compact Objects   ■ Cosmology and Fundamental Physics
☐ Stars and Stellar Evolution ☐ Resolved Stellar Populations and their Environments
☐ Galaxy Evolution   ☐ Multi-Messenger Astronomy and Astrophysics

Principal Author:
Name: Alex Kim
Institution: Physics Division, Lawrence Berkeley National Laboratory, 1 Cyclotron Road, Berkeley, CA, 94720
Email: agkim@lbl.gov
Phone: 1-510-486-4621

Co-authors: (names and institutions)

Abstract: In the upcoming decade cadenced wide-field imaging surveys will increase the number of identified $z < 0.3$ Type Ia supernovae (SNe Ia) from the hundreds to the hundreds of thousands. The increase in the number density and solid-angle coverage of SNe Ia, in parallel with improvements in the standardization of their absolute magnitudes, now make them competitive probes of the growth of structure and hence of gravity. The peculiar velocity power spectrum is sensitive to γ, which captures the effect of gravity on the linear growth of structure through the relation $f = \Omega_M^\gamma$. In the next decade the peculiar velocities of SNe Ia in the local $z < 0.3$ Universe will provide a measure of γ with as low as 0.01 precision that can definitively distinguish between General Relativity and leading models of alternative gravity.

Testing Gravity Using Type Ia Supernovae Discovered by Next Generation Wide Field Imaging Surveys

A. G. Kim,[1] G. Aldering,[1] P. Antilogus,[2] S. BenZvi,[3] H. Courtois,[4] T. Davis,[5] S. Gontcho A Gontcho,[3]
R. Graziani,[6] C. Harper,[1] C. Howlett,[7] D. Huterer,[8] C. Ju,[1] P.-F. Leget,[2] E. V. Linder,[1] P. McDonald,[1]
J. Nordin,[9] S. Perlmutter,[1, 10] N. Regnault,[2] M. Rigault,[4] A. Složar,[11] and others

[1] *Physics Division, Lawrence Berkeley National Laboratory, 1 Cyclotron Road, Berkeley, CA, 94720*
[2] *Laboratoire de Physique Nucléaire et de Hautes Energies, Sorbonne Université, CNRS-IN2P3, 4 Place Jussieu, 75005 Paris, France*
[3] *Department of Physics and Astronomy, University of Rochester, Rochester, NY 14627, USA*
[4] *Université de Lyon, F-69622, Lyon, France; Université de Lyon 1, Villeurbanne; CNRS/IN2P3, Institut de Physique Nuclaire de Lyon, France*
[5] *School of Mathematics and Physics, University of Queensland, Brisbane, QLD 4072, Australia*
[6] *Université Clermont Auvergne, CNRS/IN2P3, Laboratoire de Physique de Clermont, F-63000 Clermont-Ferrand, France*
[7] *International Centre for Radio Astronomy Research, The University of Western Australia, Crawley, WA 6009, Australia*
[8] *Department of Physics, University of Michigan, 450 Church Street, Ann Arbor, MI 48109, USA*
[9] *Institut fur Physik, Humboldt-Universitat zu Berlin, Newtonstr. 15, 12489 Berlin, Germany*
[10] *Department of Physics, University of California Berkeley, 366 LeConte Hall MC 7300, Berkeley, CA, 94720-7300*
[11] *Brookhaven National Laboratory, Physics Department, Upton, NY 11973, USA*

ABSTRACT

In the upcoming decade cadenced wide-field imaging surveys will increase the number of identified $z <$ 0.3 Type Ia supernovae (SNe Ia) from the hundreds to the hundreds of thousands. The increase in the number density and solid-angle coverage of SNe Ia, in parallel with improvements in the standardization of their absolute magnitudes, now make them competitive probes of the growth of structure and hence of gravity. The peculiar velocity power spectrum is sensitive to γ, which captures the effect of gravity on the linear growth of structure through the relation $f = \Omega_M^\gamma$. In the next decade the peculiar velocities of SNe Ia in the local $z < 0.3$ Universe will provide a measure of γ with as low as 0.01 precision that can definitively distinguish between General Relativity and leading models of alternative gravity.

1. INTRODUCTION

In the late 1990's, Type Ia supernovae (SNe Ia) were used as distance probes to measure the homogeneous expansion history of the Universe. The remarkable discovery that the expansion is accelerating has called into question our basic understanding of the gravitational forces within the Universe. Either it is dominated by a "dark energy" that is gravitationally repulsive, or General Relativity is inadequate and needs to be replaced by a modified theory of gravity. It is only appropriate that in the upcoming decade, with their sheer numbers, solid-angle coverage, and improved distance precisions, SNe Ia will provide measurements of the *inhomogeneous* motions of structures in the Universe that will provide an unmatched test of whether dark energy or modified gravity is responsible for the accelerating expansion of the Universe.

In the next decade, SNe Ia will be used as peculiar-velocity probes to measure the influence of gravity on structure formation within the Universe. The peculiar velocity power spectrum is sensitive to the growth of structure as $P_{vv} \propto (fD)^2$, where D is the linear growth factor and $f \equiv \frac{d \ln D}{d \ln a}$ is the linear growth rate (Hui & Greene 2006; Davis et al. 2011).[1] The ΛCDM prediction for the $z = 0$ peculiar velocity power spectrum is shown in Figure 1. The growth of structure depends on gravity, indeed Linder & Cahn (2007) find that General Relativity, $f(R)$, and DGP gravity follow the relation $f \approx \Omega_M^\gamma$ with $\gamma = 0.55, 0.42, 0.68$ respectively (see Huterer et al. 2015, for a review of these gravity models within a cosmological context). Adopting this parameterization to model gravity, peculiar velocity surveys are sensitive to $fD = \Omega_M^\gamma \exp\left(\int_a^1 \Omega_M^\gamma d \ln a\right)$, whose prediction for ΛCDM is plotted in Figure 2 of Linder (2013).[2]

---

[1] To be precise, the peculiar velocity power spectrum also depends on the Hubble parameter as $P_{vv} \propto (HfD)^2$. A supernova survey measures luminosity distance fluctuations $\delta_{d_L} = (d_L - \bar{d}_L(z))/\bar{d}_L(z)$, where d_L is the observed distance and $\bar{d}_L(z)$ is the expected distance at the observed redshift z. To first order in peculiar velocity along the line of sight v, $\delta_{d_L} = v\left(1 - \frac{1}{Hd_L(z)}\right) \approx -\frac{v}{Hd_L(z)}$ at low redshift. The H-dependences of P_{vv} and the conversion from distances to velocities cancel, making peculiar velocity surveys sensitive to $(fD)^2$.

[2] The parameter σ_8, the standard deviation of overdensities in $8h^{-1}$Mpc spheres, is commonly used in place of D to normalize the overall amplitude of overdensities, so the standard parameterization used by the community is $f\sigma_8$.
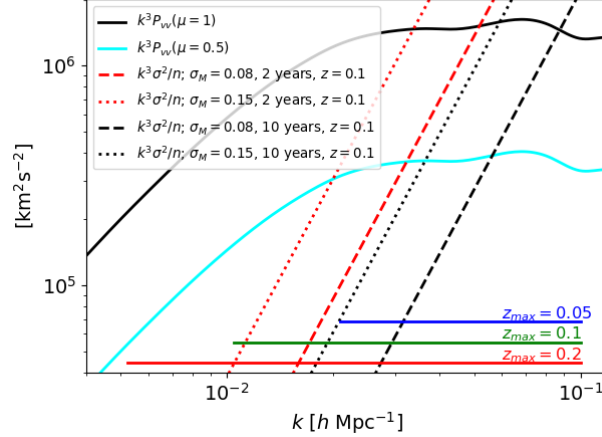
Figure 1. Volume-weighted peculiar velocity power spectrum $k^3 P_{vv}(z=0)$ for $\mu = 1, 0.5$ (solid black, cyan) as predicted for General Relativity in the linear regime. Overplotted are volume-weighted peculiar velocity shot-noise $k^3 \sigma^2/n$ at $z = 0.1$ expected from 2- and 10-year (red, black) supernova densities, 0.08 and 0.15 mag (dashed, dotted) intrinsic magnitude dispersions. The bottom solid horizontal lines show the approximate range of k expected to be used in surveys with corresponding redshift depths z_{max}.

Peculiar velocity surveys have already been used to measure fD, though not to a level where gravity models can be precisely distinguished. Adams & Blake (2017) use 6dFGS peculiar velocities using the Fundamental Plane method to get a 15% uncertainty in fD at $z \approx 0$ using combined density and velocity information. The upcoming TAIPAN survey will obtain Fundamental Plane galaxies with densities of $n_g \sim 10^{-3} h^3 \, \mathrm{Mpc}^{-3}$, and the WALLABY+WNSHS surveys will obtain Tully-Fisher galaxies at densities $n_g \sim 2 \times 10^{-2} - 10^{-4} h^3 \, \mathrm{Mpc}^{-3}$ from $z = 0 - 0.1$ covering 75% of the sky. These surveys combined are projected to have 3% fD uncertainties (Howlett et al. 2017b). (For reference, DESI projects 10% precision of fD at $z \approx 0.3$ using Redshift Space Distortions (RSD) alone.) Existing SN Ia samples have been used to test and ultimately find spatial correlations in peculiar velocities that may be attributed to the growth of structure (Gordon et al. 2007; Abate & Lahav 2008; Johnson et al. 2014; Huterer et al. 2015, 2017).

Two advances in the upcoming decade will make SN Ia peculiar velocities more powerful. First, the precision of SN Ia distances can be improved. The commonly-used empirical 2-parameter SED model yields absolute magnitude dispersion $\sigma_M \gtrsim 0.12$ mag. However, SNe transmit more information than just the light-curve shape and single color used in current SN models. Recent studies indicate that with the right data, SN absolute magnitudes can be calibrated to $\sigma_M \lesssim 0.08$ mag (see e.g. Barone-Nugent et al. 2012; Fakhouri et al. 2015). Though not yet established, it is anticipated that such a reduction in intrinsic dispersion comes with a reduction in the magnitude bias correlated with host-galaxy properties that is observed using current calibrations. One such SN is worth $\gtrsim 25$ galaxies with 0.4 mag absolute magnitude uncertainty. Secondly, in the upcoming decade cadenced wide-field imaging surveys such as ZTF and LSST will increase the number of identified $z < 0.3$ Type Ia supernovae (SNe Ia) from the hundreds to the hundreds of thousands; over the course of 10-years, LSST will find $\sim 150,000$ $z < 0.2$, $\sim 520,000$ $z < 0.3$ SNe Ia for which good light curves can be measured, corresponding to a number density of $n \sim 5 \times 10^{-4} h^3 \, \mathrm{Mpc}^{-3}$. This sample has comparable number density and more galaxies at deeper redshifts than projected by WALLABY and TAIPAN.

Given these two advances, supernovae discovered by wide-field searches in the next decade will be able to stringently constrain the growth of structure in the low-redshift Universe. For example, over the course of a decade a SN survey relying on LSST discoveries plus spectroscopic redshifts can produce find 4–14% uncertainties in fD in 0.05 redshift bins from $z = 0$ to 0.3, cumulatively giving 2.2% uncertainty on fD within this interval, where at $0 < z < 0.2$ most of the probative power comes from peculiar velocities and at higher redshifts from RSD (Howlett et al. 2017a).

2. TESTING GRAVITY WITH PECULIAR VELOCITY SURVEYS

While the growth rate fD can be used to test several aspects of physics beyond the standard cosmological model (e.g. dark matter clustering, dark energy evolution), our scientific interest here is in probing gravity so we here focus on the growth index γ. To illustrate the distinction, $\frac{d(\ln fD)}{d\gamma} = \ln \Omega_M + \int \Omega_M^\gamma \ln \Omega_M \, d\ln a \approx -1.68, -0.75, -0.37$ at $z = 0, 0.5, 1.0$ respectively in ΛCDM; two surveys with the same fractional precision in fD will have different precision

in γ, with the one at lower redshift providing the tighter constraint. In this section, we focus on how well peculiar velocity surveys in the upcoming decade can measure γ and the sensitivity of the measurement on survey parameter choices.

We project uncertainties on the growth index, σ_γ for a suite of idealized surveys using a Fisher matrix analysis similar to that of Howlett et al. (2017a,b) (there is an alternative approach using an estimator for the mean pairwise velocity Bhattacharya et al. 2011). The Fisher information matrix is

$$F_{ij} = \frac{\Omega}{8\pi^2} \int_0^{r_{max}} \int_{k_{min}}^{k_{max}} \int_{-1}^{1} r^2 k^2 \text{Tr}\left[C^{-1} \frac{\partial C}{\partial \lambda_i} C^{-1} \frac{\partial C}{\partial \lambda_j} \right] d\mu\, dk\, dr \tag{1}$$

where

$$C(k,\mu) = \begin{bmatrix} P_{\delta\delta}(k,\mu) + \frac{1}{n} & P_{v\delta}(k,\mu) \\ P_{v\delta}(k,\mu) & P_{vv}(k,\mu) + \frac{\sigma^2}{n} \end{bmatrix} \tag{2}$$

and the two parameters considered are $\lambda \in \{\gamma, bD\}$. The parameter dependence enters through $(fD)(\gamma)$ in the relations $P_{vv} \propto (fD\mu)^2$, the SN Ia host-galaxy overdensity power spectrum $P_{\delta\delta} \propto (bD + fD\mu^2)^2$, and the galaxy-velocity cross-correlation $P_{vg} \propto (bD + fD\mu^2)fD$, where b is the galaxy bias and μ is the cosine of the angle between the k-mode and the line of sight. While the bD term does contain information on γ, its constraining power is not used here. The uncertainty in γ is $\sigma_\gamma = \sqrt{(F^{-1})_{\gamma\gamma}}$. Non-GR models may also predict a change in the scale-dependence of the growth or non-constant γ, such observations provide additional leverage in probing gravity but are not considered.

The uncertainty σ_γ of a survey depends on its solid angle Ω, depth given by the comoving distance out to the maximum redshift $r_{max} = r(z_{max})$, duration t through $n = \epsilon\phi t$ where ϕ is the observer-frame SN Ia rate and ϵ is the sample-selection efficiency, and the intrinsic SN Ia magnitude dispersion through $\sigma \approx (\frac{5}{\ln 10} \frac{1+z}{z})^{-1} \sigma_M$. An analysis in which the RSD and velocity surveys are treated independently sets the off-diagonal elements of C to zero.

We consider peculiar velocity surveys for a range of redshift depths z_{max} for survey durations of $t = 2$ and 10 years. The other survey parameters $\Omega = 3\pi$, $\epsilon = 0.65$, $\sigma_M = 0.08$ mag are fixed. The k-limits are taken to be $k_{min} = \pi/r_{max}$ and $k_{max} = 0.1\, h\,\text{Mpc}^{-1}$. The sample-selection efficiency ϵ is redshift-independent, i.e. the native redshift distribution is not sculpted. The input bias of SN Ia host galaxies is set as $b = 1.2$.

All the surveys considered provide meaningful tests of gravity. The projected uncertainty in γ achieved by the suite of surveys are shown in Figure 2. The primary analysis of interest uses overdensities (RSD), peculiar velocities, and their cross-correlations. The short and shallow, 2-year, $z_{max} = 0.1$ survey has $\sigma_\gamma \sim 0.038$, which can distinguish between General Relativity, $f(R)$, and DGP gravities at the $> 3\sigma$ level. The 10-year survey performance asymptotes at $z_{max} \sim 0.2$ at a precision of $\sigma_\gamma \sim 0.01$. Figure 2 also shows uncertainties based on two other analyses, one that only uses peculiar velocities, and one that combines independent RSD and peculiar velocity results. Peculiar velocities alone can account for much of the probative power of the surveys. RSD alone do not provide significant constraints. However, considering RSD and velocity cross-correlations decreases σ_γ by $\sim 20\%$. The implication is that there are important k-modes that are sample variance limited either in overdensity and/or peculiar velocity who benefit from the sample-noise suppression engendered by cross-correlations.

Survey performance is examined in more detail by considering how σ_γ (using RSD, peculiar velocities, and their cross-correlations) changes with respect to the survey parameters Ω, z_{max}, t, and σ_M, and also with respect to differential redshift bins within a given survey. Though not directly a survey parameter, we also examine changes with respect to k_{max}.

The dependence on the uncertainty in the growth index on the survey parameters is as follows:

Solid Angle Ω: The Fisher Matrix F is proportional to the survey solid angle Ω so $\sigma_\gamma \propto \Omega^{-1/2}$.

Differential Redshift Bin z: Certain redshifts constrain γ more strongly than others. If at a given moment of a survey we had a set of SNe Ia from which to choose, it turns out the one with the lowest redshift would be preferred. This is demonstrated to be the case at the end of both 2- and 10-year surveys with $z_{max} = 0.2$. The leftpanel of Figure 3 shows $|\partial \sigma_\gamma / \partial z|$, which for both surveys monotonically decreases from $z = 0.01$ out to $z = 0.2$. If we had to sculpt the distribution (say due to limited follow-up resources), the preference would be to cut out the highest redshift bins resulting in a decreased z_{max}. The optimal redshift distribution is thus the unsculpted SN-discovery distribution truncated by z_{max}.

Redshift Depth z_{max}: Increasing the survey redshift depth increases the γ precision. The differential improvement in σ_γ plateaus at $z_{max} \sim 0.2$ as seen in Figure 2.
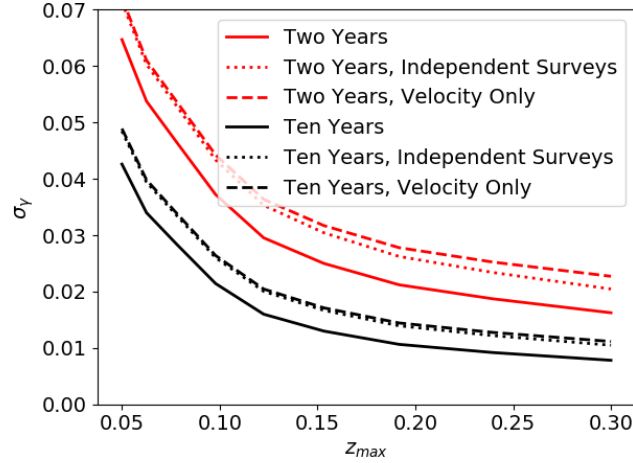
Figure 2. The projected uncertainty in γ, σ_γ, achieved by two- (red) and ten-year (black) surveys of varying depth z_{max}. For each survey uncertainties are based on three types of analyses, one that only uses peculiar velocities (dashed), one that uses both RSD and peculiar velocities independently (dotted), and one that uses both RSD, peculiar velocities, and their cross-correlation (solid).
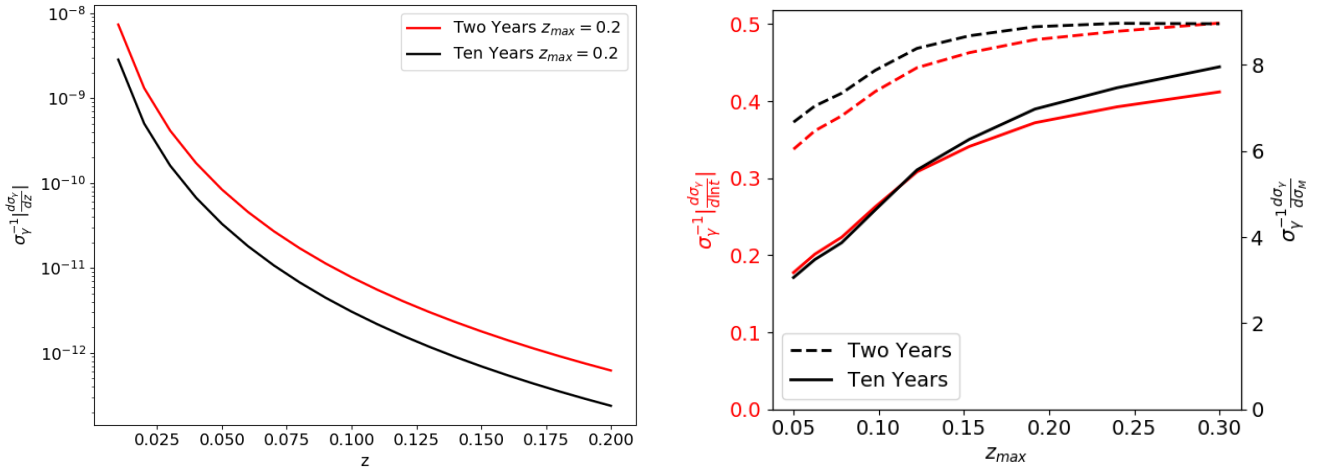

Figure 3. Left: $|\partial\sigma_\gamma/\partial z|$ after two and ten years for a survy with limiting depth $z_{max} = 0.2$. Right: $\sigma_\gamma^{-1}|\partial\sigma_\gamma/\partial \ln t|$ (red) and $\sigma_\gamma^{-1}\partial\sigma_\gamma/\partial\sigma_M$ (black) each as a function of z_{max} for two- (dashed) and ten-year (solid) surveys.

Survey duration t; Intrinsic Magnitude Dispersion σ_M: An increased survey duration accumulates more supernovae, decreasing shot noise and increasing the precision in γ for all the surveys considered. The surveys we consider have varying relative contributions of sample variance and shot noise: those that have a larger shot-noise contribution, shorter surveys and those with higher z_{max} (because of the higher σ), benefit more from extending survey duration. These trends are shown in the left panel of Figure 3, which plots $\sigma_\gamma^{-1}|\partial\sigma_\gamma/\partial \ln t|$ as a function of z_{max} for two- and ten-year surveys. Like survey duration, intrinsic magnitude dispersion is related to survey performance through the shot noise and thus has a similar relationship with σ_γ. This is evident in the plot of $\sigma_\gamma^{-1}\partial\sigma_\gamma/\partial\sigma_M$ also shown in the left panel of Figure 3.

Minimum length scale, maximum wavenumber k_{max}: There is a minimum length scale at which density and velocity distributions are reliably predicted from theory. Changes in this scale engender fractional changes in the γ precision as $\sigma_\gamma^{-1}\partial\sigma_\gamma/\partial k_{max} = 0.0050$ at $k_{max} = 0.1h\,\mathrm{Mpc}^{-1}$, which is survey-independent.

The condition of sample variance–shot noise equality of a k-mode is now examined. This is important in tuning survey design because, as mentioned above, the range of surveys of interest have different relative contributions of

sample variance and shot noise. The RSD measurement is sample variance limited, as within a few years supernova discoveries from the rest-frame volumetric rate of $\phi = 7.84 \times 10^{-5} h^3 \, \mathrm{Mpc}^{-3} \, \mathrm{yr}^{-1}$ make shot noise unimportant. For peculiar velocities, the contributions of P_{vv} and σ^2/n at $z = 0.1$ for $\sigma_M = 0.08, 0.15$ mag with number densities from 2- and 10-year surveys can be compared using Figure 1. For these survey scenarios, sample variance and shot-noise equality occurs at a k within the range that carries the most signal; both sample variance and shot-noise limited modes contribute to the constraints. If k_{max} were to decrease moderately some of the surveys could become sample variance limited, whereas increases in k_{max} introduce additional shot-limited modes.

3. ELEMENTS OF A PECULIAR VELOCITY SURVEY

A successful peculiar velocity survey must accomplish several things, not just measure distances and host-galaxy redshifts. These elements are as follows:

SNe Must Be Discovered: Cadenced wide-field imaging surveys have proven to be efficient SN Ia discovery machines. ZTF and LSST are examples, but not the sole representatives, of current and future surveys that will generate high surface-densities of SNe Ia n over a large solid angle Ω. For example, LSST is expected to discover all $z < 0.3$ SNe Ia before maximum light in its active Wide Fast Deep (WFD) survey area.

SNe Ia Must Be Classified: Cadenced wide-field imaging surveys discover SNe Ia together with a background of other transient events. The peculiar velocity analysis is performed using a subset of all of these transients, with the intrinsic magnitude dispersion dependent on sample selection criteria. Tailored SN Ia subsets and pure SN Ia samples will have lower σ_M compared to samples that suffer from non-Ia contamination. Spectroscopic classification can ensure the purity of the analysis sample. SNe Ia are defined based on spectroscopic features, through the absence of Hydrogen and the presence of the 6150 Å Silicon P-Cygni feature. SNIFS and SED Machine are examples of single-object spectrographs built with the purpose of classifying transients discovered in imaging surveys (the low surface density of active low-z transients makes MOS superfluous). Photometric classification is an alternative approach, which benefits from the light-curve data already in hand from the search. The level of σ_M that can be achieved, SN Ia completeness, and the effect of classification-distance covariance are subjects of active research. Photometric classification benefits from having spectroscopic redshifts.

Host-galaxies Need Precise Redshifts: Peculiar velocities come from the difference between host-galaxy and cosmological redshifts. Host redshift uncertainties need to be $< 0.5\%$ in order not to contribute significantly to the error budget. We thus conclude that there is the need for spectroscopic $R > 200$ host-galaxy redshifts. These redshifts could come naturally from galaxy signal in the spectroscopic transient classification if the spectrograph had sufficient resolution. Alternatively, moderate-resolution (bright-)galaxy redshift surveys (e.g. DESI, 4MOST) can provide multiplexed observations of a significant fraction of nearby SN hosts before discovery or after transient light has faded away.

SNe Ia Need Precise Distances: SN Ia distances, along with their measured redshifts, are required to infer the peculiar velocities of their hosts. Distances are calculated from multi-band light curves, redshifts (when available), SN spectroscopic features, and host-galaxy properties. Distance uncertainties here have been characterized by magnitude dispersion σ_M, which includes both measurement uncertainty and intrinsic magnitude dispersion. The latter depends on the data-quality and methodology used to calculate distances. For the same supernovae, the intrinsic distance dispersion derived from a dataset with sparse light curves, a small number of bands, limited wavelength coverage, and lacking spectral-feature measurements is larger compared to the dispersion derived from a broader dataset with dense light curves, a large number of bands, broad wavelength coverage, and with spectral-feature measurements. Historically surveys with two or three well-sampled optical light curves obtained $\sigma_M \approx 0.15$ mag, with dense, $griz$-band optical light curves DES (Brout et al. 2018) gets $\sigma_M \approx 0.10$ mag, standardization studies show that supplemental infrared data (Barone-Nugent et al. 2012) or spectrophotometry at peak brightness (Fakhouri et al. 2015) are projected to give $\sigma_M \lesssim 0.08$ mag. The improvement between $\sigma_M = 0.08$ and 0.15 mag dispersions is equivalent to a factor of 3.52 in number density, or equivalently in survey duration.

As a point of reference, a practically complete (accounting for temporal observing gaps) discovery up to $z_{max} = 0.2$ would have $\sim 150,000$, $r \lesssim 20.5$ mag targets over 10 years. Focusing on low-redshift supernovae mitigates several important uncertainties associated with the high-z SN Ia cosmology. The measurement is relatively insensitive to absolute color calibration, due to the limited range of *observer* wavelengths used to standardize restframe distance moduli. Depending on which cameras are used to derive distances, instrumental, as opposed to absolute, calibration may be sufficient. The progenitor population is not expected to evolve significantly in the $0.01 < z < 0.2$ Universe.

4. CONCLUSIONS

In the next decade, the high number of SN discoveries together with improved precision in their distance precisions will make $z < 0.2$ SNe Ia, more so than galaxies, powerful probes of gravity through their effect on the growth of structure. A peculiar velocity survey must discover, classify, and get distances of SNe Ia, as well as obtain redshifts of their host galaxies. Choices in survey design impact the precision obtained on the growth index γ. No other probe of growth of structure or tracer of peculiar velocity can provide comparable precision on γ in the next decade. SN Ia peculiar velocity surveys are of the highest scientific interest and we encourage the community to develop aggressive surveys in the pursuit of testing General Relativity and probing gravity.

REFERENCES

Abate, A., & Lahav, O. 2008, MNRAS, 389, L47, doi: 10.1111/j.1745-3933.2008.00519.x

Adams, C., & Blake, C. 2017, MNRAS, 471, 839, doi: 10.1093/mnras/stx1529

Barone-Nugent, R. L., Lidman, C., Wyithe, J. S. B., et al. 2012, MNRAS, 425, 1007, doi: 10.1111/j.1365-2966.2012.21412.x

Bhattacharya, S., Kosowsky, A., Newman, J. A., & Zentner, A. R. 2011, PhRvD, 83, 043004, doi: 10.1103/PhysRevD.83.043004

Brout, D., Scolnic, D., Kessler, R., et al. 2018, arXiv e-prints. https://arxiv.org/abs/1811.02377

Davis, T. M., Hui, L., Frieman, J. A., et al. 2011, ApJ, 741, 67, doi: 10.1088/0004-637X/741/1/67

Fakhouri, H. K., Boone, K., Aldering, G., et al. 2015, ApJ, 815, 58, doi: 10.1088/0004-637X/815/1/58

Gordon, C., Land, K., & Slosar, A. 2007, Phys. Rev. Lett., 99, 081301, doi: 10.1103/PhysRevLett.99.081301

Howlett, C., Robotham, A. S. G., Lagos, C. D. P., & Kim, A. G. 2017a, ApJ, 847, 128, doi: 10.3847/1538-4357/aa88c8

Howlett, C., Staveley-Smith, L., & Blake, C. 2017b, MNRAS, 464, 2517, doi: 10.1093/mnras/stw2466

Hui, L., & Greene, P. B. 2006, PRD, 73, 123526, doi: 10.1103/PhysRevD.73.123526

Huterer, D., Shafer, D. L., & Schmidt, F. 2015, JCAP, 12, 033, doi: 10.1088/1475-7516/2015/12/033

Huterer, D., Shafer, D. L., Scolnic, D. M., & Schmidt, F. 2017, JCAP, 5, 015, doi: 10.1088/1475-7516/2017/05/015

Huterer, D., Kirkby, D., Bean, R., et al. 2015, Astroparticle Physics, 63, 23 , doi: https://doi.org/10.1016/j.astropartphys.2014.07.004

Johnson, A., Blake, C., Koda, J., et al. 2014, MNRAS, 444, 3926, doi: 10.1093/mnras/stu1615

Linder, E. V. 2013, Journal of Cosmology and Astroparticle Physics, 2013, 031

Linder, E. V., & Cahn, R. N. 2007, Astroparticle Physics, 28, 481, doi: 10.1016/j.astropartphys.2007.09.003